Journal of the Serbian Chemical Society
JSCS-info@shd.org.rs • www.shd.org.rs/JSCS
J. Serb. Chem. Soc. 76 (2) 283–303 (2011)
JSCS–4118
UDC 546.151–128.2+546.48–128.4+ 544.723:546.57
Original scientific paper

Processes of adsorption/desorption of iodides and cadmium cations onto/from Ag(111)

VLADIMIR D. JOVIĆ*# and BORKA M. JOVIĆ#

Institute for Multidisciplinary Research, P.O. Box 33, 11030 Belgrade, Serbia

(Received 1 July, revised 23 August 2010)

Abstract: In this work, the adsorption/desorption processes of iodides and cadmium cations in the presence of iodides onto/from Ag(111) were investigated. It was shown that both processes were complex, characterized by several peaks on the cyclic voltammograms (CVs). By PeakFit analysis of the recorded CVs and subsequent fitting of the obtained peaks by the Frumkin adsorption isotherm, the interaction parameter (f) and the Gibbs energy of adsorption (ΔG_{ads}) for each adsorbed phase were determined. In the case of iodide adsorption, four peaks were characterized by negative values of f, indicating attractive lateral interaction between the adsorbed anions, while two of them possessed value of $f < -4$, indicating phase transition processes. The adsorption/desorption processes of cadmium cations (underpotential deposition – UPD of cadmium) in the presence of iodide anions was characterized by two main peaks, each of them being composed of two or three peaks with negative values of f. By the analysis of charge *vs*. potential dependences obtained either from the CVs or current transients on potentiostatic pulses, it was concluded that adsorbed iodides did not undergo desorption during the process of Cd UPD, but became replaced by Cd ad-atoms and remained adsorbed on top of a Cd layer and/or in between Cd the ad-atoms.

Keywords: Ag(111); iodide adsorption; iodide desorption; Cd underpotential deposition; phase transition.

INTRODUCTION

The first ordered iodide structures on Ag(111) emersed from dilute HI solutions were observed by Salaita *et al.*[1] using the Ultra high vacuum–electrochemical (UHV–EC) technique: one with triangular splitting of subspots in the negative potential range and the other with hexagonal splitting in the positive potential range. Several adlayer structures were also reported for iodine on Ag(111):

* Corresponding author. E-mail: vladajovic@imsi.rs
# Serbian Chemical Society member.
doi: 10.2298/JSC100701026J

scanning tunneling microscopy (STM) images of a flat adlayer of I/Ag(111) obtained in air being ascribed to the so-called ($5\times\sqrt{3}$) structure;[2–4] contracted ($\sqrt{3}\times\sqrt{3}$)R–30° adlattice detected by X-ray photoelectron spectroscopy (XPS) performed on iodine-covered Ag(111).[5] Adsorption/desorption process of iodides from iodide-containing solutions on oriented silver single crystal surfaces has been investigated by capacitance, voltammetric and surface analytical techniques.[6,7] A common characteristic of the voltammetric investigations was the presence of a broad peak at more negative potentials and a sharp peak at less negative potentials. The broad peak was ascribed to the formation of a randomly distributed adlayer at potentials negative of –0.8 V *vs*. SHE and its transformation to a ($\sqrt{3}\times\sqrt{3}$)R30° ordered structure between –0.8 and –0.13 V *vs*. SHE. Further compression of such an ordered structure into an (8×8) iodide structure, expressed by a sharp peak on the CVs, was detected at potentials slightly positive of –0.13 V *vs*. SHE.[6,7] Detailed *in situ* STM and *ex situ* low energy electron diffraction (LEED) studies of Yamada *et al*.[8] in KI buffered with KF–KOH at pH 10 and HI solutions confirmed the continuous compression of the iodide adlattice from square ($\sqrt{3}\times\sqrt{3}$ R–30°), *via* ($\sqrt{3}\,qR\beta°\times\sqrt{3}$ R–30°) ($q \approx 1$, $0 \leq \beta \leq 30$), to ($\sqrt{3}\times\sqrt{3}$)R30° with increasing electrode potential, followed by an abrupt phase transition into a rotated hexagonal ($\sqrt{3}\times\sqrt{3}$)R(30°+α°) phase at potentials more positive than the potential of the sharp peak on the CV. Their CV recorded in 0.1 mM KI + 10 mM KF + 0.1 mM KOH at a sweep rate of 5 mV s^{-1} was characterized by a nucleation loop at –0.06 V *vs*. SHE, by pair of sharp, phase transition peaks, at around –0.16 V *vs*. SHE and a pair of broad peaks between around –0.61 and –0.96 V *vs*. SHE. The pair of broad peaks possessed two pairs of small sharp peaks at potentials around –0.68 and –0.76 V *vs*. SHE. Except the ($\sqrt{3}\times\sqrt{3}$)R(30°+α°) phase detected by *in situ* STM at potentials more positive that the potential of the sharp (phase transition) peaks on the CV at around –0.16 V *vs*. SHE, all the other above-mentioned structures were detected in the so-called double layer region, between the broad and the sharp peak on the CV. The CV recorded at the same sweep rate in a solution of 0.1 mM HI possessed only a nucleation loop at –0.06 V *vs*. SHE and a pair of sharp, phase transition peaks, at around –0.16 V *vs*. SHE. From this solution, only *ex situ* LEED–Auger electron spectroscopy (LEED–AES) experiments were performed. At an emersion potential of –0.48 V *vs*. SHE, a ($\sqrt{3}\times\sqrt{3}$)R30° adlayer structure was detected; at an emersion potential of –0.28 V *vs*. SHE, a $c(p\times\sqrt{3}$ R–30°) adlayer structure with p = 0.264 was detected, while a ($\sqrt{3}\times\sqrt{3}$)R(30°+α°) phase was detected at an emersion potential of –0.1 V *vs*. SHE, positive of a phase transition peak. Hence, the appearance of different ordered structures was found to depend on the solution composition.

Underpotential deposition (UPD) of cadmium onto silver single crystals has not been studied extensively. Bort *et al*.[9] found that on a Ag(111) surface, the

UPD of Cd commenced at a potential of about –0.18V *vs*. SHE, with the formation of a ($\sqrt{3}\times\sqrt{3}$)R30° structure. The voltammetric peaks associated with this process were reversible. A second cathodic peak, observed at about –0.41 V *vs*. SHE, was reported to correspond to a monolayer deposition of Cd, while the charge associated with a third cathodic peak was consistent with that required for a second monolayer of Cd. Almost identical results were obtained in the work of Garcia *et al*.[10] By *in situ* STM, it was shown that the Cd UPD process starts with the formation of an expanded (diluted) adlayer with a superlattice structure Ag(111)–($\sqrt{3}\times\sqrt{19}$)R23.4°, being transformed to a condensed close packed Cd monolayer *via* a first order phase transition. During long time polarization in the potential range of monolayer formation, the monolayer transforms into an Ag–Cd surface alloy by place exchanging between Cd atoms and surface Ag atoms. At more negative potentials, the formation of a second Cd monolayer, with pronounced alloying between Ag and Cd, was found to occur.[10] The formation of the superlattice and both monolayers was clearly detected by *in situ* STM.[10] The kinetics of the alloying process was also investigated showing that de-alloying led to the appearance of large number of 2D islands and monoatomic deep steps, which rapidly disappeared at more positive potentials, suggesting a relatively high mobility of the surface Ag atoms under such conditions.[10] The same processes (UPD and alloying of Ag with Cd) were also investigated in a chloride--containing solution.[11] Identical conclusion were reached concerning UPD and alloying, except that it was concluded in this work that chloride ad-atoms, which are adsorbed on the silver substrate when UPD of Cd starts, did not undergo desorption. They became replaced by Cd ad-atoms and remained adsorbed and discharged on top of a Cd layer.[11]

In the present work, an attempt to investigate the adsorption/desorption process of iodides and the UPD of Cd onto Ag(111) in the presence of iodides was made.

EXPERIMENTAL

All experiments were performed in a two-compartment electrochemical cell at 25±1 °C. The single crystal electrode (Monocrystals Company, d = 0.9 cm) was sealed in epoxy resin in such a way that only the (111) disc surface was exposed to the solution. The surface area of the electrode exposed to the electrolyte was 0.636 cm^2. The counter electrode (CE) was a Pt sheet, which was placed parallel to the working electrode. The reference electrode (RE) was a saturated silver chloride electrode (Ag/AgCl). All results are given *vs*. SHE. The RE was placed in a separate compartment and connected to the working compartment by means of a Luggin capillary. Solutions of 0.1 M NaI and 0.05 M CdI_2 were made from supra pure (99.999 % – Aldrich) chemicals and extra pure UV water (Smart2PureUV, TKA).

The single crystals were prepared by a mechanical polishing procedure followed by chemical polishing in the solution containing NaCN and H_2O_2, as explained in a previous paper.[12] Before each experiment, the electrolyte was purged with high purity nitrogen (99.999 %)

for 45 min, while a nitrogen atmosphere was maintained over the solution during the experiment to prevent contamination with oxygen.

All experiments were performed using a potentiostat Reference 600 and PHE 200 software (Gamry Instruments Inc.).

The deconvolution of the experimentally recorded peaks on the CVs was performed by the computer program PeakFit for Win32, version 4.05 (AISN Software). All fits were performed with the Gauss + Lorenz Amp function. With this function it was possible to vary the width and shape of the resulting peaks. In such a way, it was possible to obtain a fitting curve identical to the experimental one.

RESULTS AND DISCUSSION

Iodide adsorption/desorption in 0.1 M NaI

CV recorded at a sweep rate of 200 mV s^{-1} in 0.1 M NaI is presented in Fig. 1. The process of iodide adsorption/desorption is characterized by one pair of broad peaks, composed of several small, sharp peaks in the negative potential region (from ≈ –0.7 to ≈ –1.0 V) and one pair of sharp peaks at less negative potentials (around –0.16 V). It is important to note that in the investigated solution (pH around 7), the process of hydrogen evolution should commence at about –0.42 V *vs.* SHE. Taking into account a certain overvoltage for hydrogen evolution onto an Ag electrode, this value should be more negative (by about 0.2–0.3 V). According to the CVs presented in the work of Yamada *et al.*[8] in a solution containing 0.1 mM KI + 10 mM KF + 0.1 mM KOH (pH 10) at the sweep rate of 5 mV s^{-1}, the CV started declining to the cathodic direction at about –0.68 V *vs.* SHE (Fig. 1A), while in a solution containing 0.1 mM HI (pH 4.3), the process of iodide adsorption could not be seen since the massive hydrogen evolution (at a

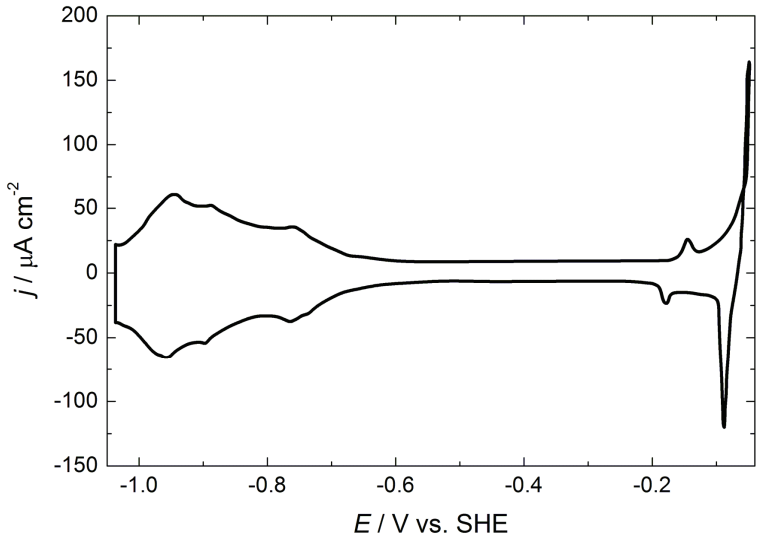

Fig. 1. CV of Ag(111) in 0.1 M NaI recorded at a sweep rate v = 200 mV s^{-1}.

sweep rate of 5 mV s^{-1}) started already at about –0.6 V *vs.* SHE (Fig. 1B). In order to avoid simultaneous hydrogen evolution, taking into account that the processes of anion adsorption are much faster, it was necessary to apply sweep rates higher than 100 mV s^{-1}. Hence, on the CVs recorded at the sweep rates ≥ 100 mV s^{-1}, the declining of the CVs to the cathodic direction could be avoided and well-defined CVs down to –1.0 V were recorded (see Figs. 1 and 4a), with no charge of hydrogen evolution contributing to the charge required for iodide adsorption. The sudden increase of the cathodic current density corresponding to the hydrogen evolution was recorded immediately after the cathodic limit on the presented CVs (not presented in Figs. 1 and 4a). As can be seen in Fig. 1, at potentials close to zero, an anodic nucleation loop was obtained as a result of the beginning of 3D nucleation of AgI, as was the case in other investigations.[1–8] If the anodic potential limit was set to more positive values, a large amount of AgI (probably 3D islands) would form on the Ag(111) surface and its original orientation would be destroyed, causing significant changes on the CV of the iodide adsorption/desorption process (a similar effect was recorded for AgCl formation,[13] but this effect is much more pronounced in the case of AgI).

By integrating the surface under the cathodic and anodic parts of the CV shown in Fig. 1, the corresponding charge *vs.* potential curves were obtained, which are presented in Fig. 2. As can be seen, mirror-like dependences were obtained with a maximum anodic charge (Q_a) of ≈ 90 μC cm^{-2} and a maximum cathodic charge (Q_c) of ≈ 97 μC cm^{-2}. Taking into account that the theoretical charge (assuming complete charge transfer) for an $(\sqrt{3}\times\sqrt{3})$R30° iodide ad-

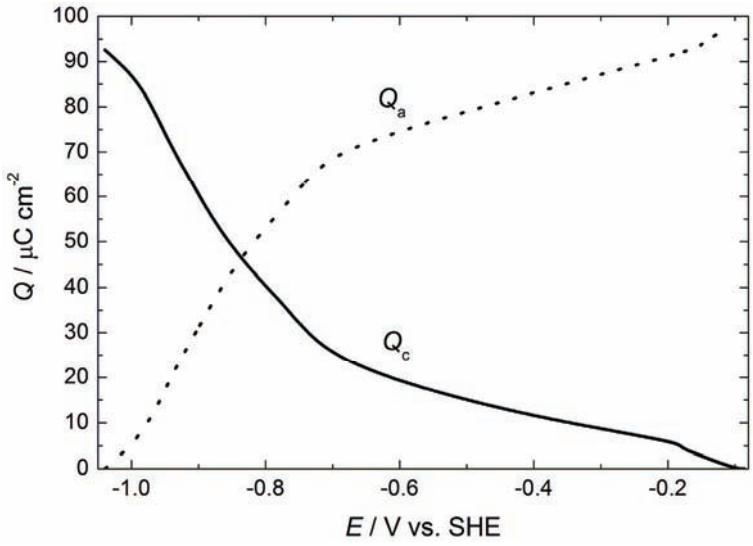

Fig. 2. Cathodic (Q_c) and anodic (Q_a) charges as a function of the potential obtained by integration of the corresponding parts (from –1.02 to –0.1 V) of the CV presented in Fig. 1.

layer[1–8] amounts to 74 μC cm^{-2}, it seems that this adlayer forms under the broad peak (sharp increase of the Q_a *vs.* E up to about 70 μC cm^{-2} at a potential of ≈ –0.65 V), with its further compression expressed by the slow increase of the anodic charge. Such behavior is in accordance with the findings of Yamada *et al.*,[8] although their solution was composed of a mixture of iodide, fluoride and hydroxide of mM concentrations.

In order to investigate more precisely the process of iodide adsorption, the anodic part of the CV shown in Fig. 1 (as well as in Fig. 4a) was analyzed by the PeakFit program. The results of such an analysis are presented in Fig. 3. As can be seen in Fig. 3a, all peaks obtained by deconvolution overlap, indicating that during this dynamic process, different structures could start forming during the formation of some other structure. The sum of all peaks, A, A1–A4 gives the curve presented with solid line showing the best fit of this part of the experimental curve (○). This is most likely the reason why *in situ* STM could not detect any ordered structure in this potential region[8] and ordered structures were detected at more positive potentials in the "double layer region". Simultaneously, the process of "random adsorption" (characterized by peak A) occurs in the potential range between –1.0 and –0.7 V, which is most likely adsorption of iodides at the monoatomic steps, since this type of adsorption is energetically favorable and usually finishes when the whole electrode surface is covered with the adsorbed anions. Hence, all these processes occur more or less simultaneously and deconvolution of the recorded anodic *j*–*E* curve was necessary for their differentiation. After deconvolution, five peaks were obtained. Each of them is considered as a CV of a single adsorption process and each peak was separately analyzed. After integration of the anodic *j*–*E* curve for each peak, the total charge for this particular peak was obtained and this value was used as Q_{max}. θ was calculated as Q/Q_{max}. In such a way, θ varied from 0 to 1 for each peak. The sharp peak at less negative potentials (around –0.16 V) could be fitted with only one peak B. Adsorption isotherms (θ *vs.* E dependences, presented with squares and circles) for peaks A and B are shown in Fig. 3b. Those for the peaks A1–A4 (presented with squares, circles and triangles) are shown in Fig. 3c. All adsorption isotherms presented in Figs. 3b and 3c were fitted with the Frumkin adsorption isotherm (fitting results are presented with solid, dashed, dotted, and dash–dot lines) expressed by the Equation:[14]

$$E = \frac{RT}{F}\left\{\ln\left(\frac{\theta}{1-\theta}\right) + f\theta - \ln\left(K_{\text{ads},\theta\to 0}c_0\right)\right\} \quad (1)$$

where $K_{\text{ads},\theta\to 0}c_0$ is the equilibrium constant for adsorption, $f = r/\text{RT}$ representing interaction parameter (with r being the rate of change of the Gibbs energy of adsorption with coverage), c_0 concentration of anions, while R, T and F have their usual meaning.

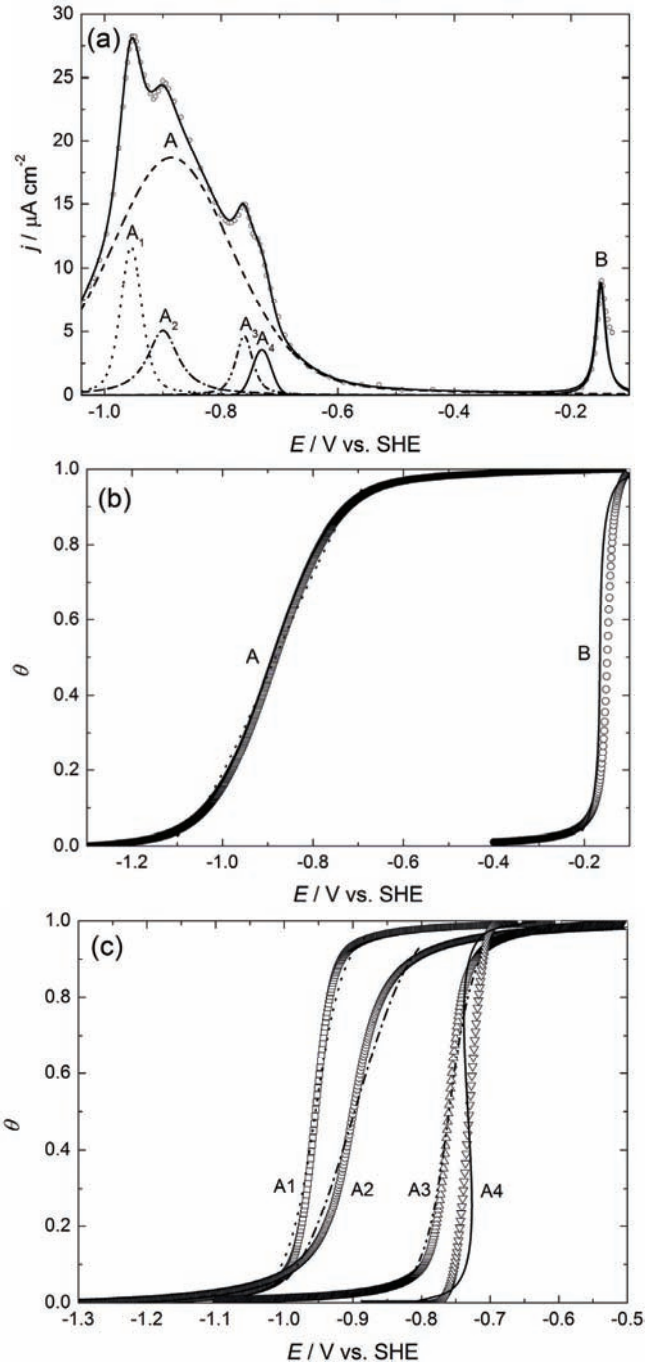

Fig. 3. a) Anodic part of the CV presented in Fig. 4a (v = = 100 mV s^{-1}): ○ – experimental curve; solid line – curve obtained by the PeakFit procedure; all peaks obtained by this procedure are marked with A, A1–A4 and B; b) adsorption isotherms obtained by the analysis of the corresponding peaks in (a): □ – experimental curve for peak A; dotted line – curve obtained after fitting the θ *vs.* E dependence for peak A with the Frumkin adsorption isotherm; ○ – experimental curve for peak B; solid line – fitting curve; c) adsorption isotherms obtained by analysis of the corresponding peaks in (a): □ – experimental curve for peak A1; dotted line – fitting curve; ○ – experimental curve for peak A2; dash-dot line – fitting curve; △ – experimental curve for peak A3; dash-dot-dot line – fitting curve; ▽ – experimental curve for peak A4; solid line – fitting curve.

The values of the Gibbs energies of adsorption were obtained from a following relation:[14]

$$\Delta G_{\text{ads}} = -2.3RT \log K_{\text{ads},\theta\to 0} \quad (2)$$

The best fits for the isotherms presented in Figs. 3b and 3c were obtained with the parameters given in Table I. As could be expected, the adsorption isotherm for peak A (Fig. 3b) is characterized by a high positive value of the interaction parameter (f = 9.1), indicating repulsive lateral interaction between the adsorbed iodides. The adsorption equilibrium constant is also very high, 9.4×10^{20} and an accordingly high negative value of the Gibbs energy of adsorption is obtained (–119.8 kJ mol^{-1}). The interaction parameter f of the adsorption isotherm for the peak B, which, according to Yamada *et al.*[8] represents the phase transition of the $(\sqrt{3}\times\sqrt{3})$R30° adlayer into the rotated hexagonal $(\sqrt{3}\times\sqrt{3})$R(30°+α°) phase, possess a negative value (f = –4.3), confirming the attractive lateral interaction between the adsorbed iodide anions and the phase transition process, since it is more negative than the critical value of f for the phase transition (f = –4).[14] The adsorption equilibrium constant is by several orders of magnitude lower than that for peak A, 1.1×10^{6} and, accordingly, a much smaller negative value of the Gibbs energy of adsorption is obtained (–34.5 kJ mol^{-1}), Table I. Taking into account the shape of the CV (there are no peaks between –0.6 and –0.2 V, this part practically represents the double layer region), it seems reasonable to ascribe peak B to the process of phase transition of the $(\sqrt{3}\times\sqrt{3})$R30° adlayer into the rotated hexagonal $(\sqrt{3}\times\sqrt{3})$R(30°+α°) phase. The values of f for peaks A1, A3 and A4 are also negative, indicating attractive lateral interaction between the adsorbed anions, but only one, for peak A4, is more negative than f = –4, confirming the phase transition process at the end of the broad peak between –1.0 and –0.7 V. Taking into account that continuous compression of the iodide adlattice from square $(\sqrt{3}\times\sqrt{3}$ R–30°), *via* $(\sqrt{3}\,qR\beta$ °$\times\sqrt{3}$ R–30°) ($q \approx 1$, $0 \le \beta \le$ ≤ 30), to $(\sqrt{3}\times\sqrt{3})$R30° occurs with increasing electrode potential, it seems reasonable to ascribe peaks A1, A3 and A4 to the processes of the formation of these three ordered adlayers. While their compression is a dynamic process accompanied with the adsorption of new anions, it appears that the final step, the formation of the $(\sqrt{3}\times\sqrt{3})$R30° adlayer represents a phase transition process, which is in good agreement with an *in situ* STM analysis.[8] Peak A2 should also represent a process of iodide adsorption in which some disordered – random structure, characterized by a positive value of f is formed, most probably at the beginning of the formation of the ordered structure characterized by peak A3. This is often the case in anion adsorption.[15] The main difference between the results and those presented previously[8] is the potential region in which the abovementioned ordered structures (peaks A1, A3, and A4) were formed. From the present analysis, it appears that these three structures were formed under the

broad peak, at more negative potentials than those in the literature.[8] There are two reasons for such a difference: first, STM can detect only stable, ordered structures and during the dynamic change of the adsorbing conditions under the broad peak, the formation of ordered structures most likely cannot be seen; second, the solution for *in situ* STM study[8] contained KOH at the same concentration as KI, with the adsorption of OH^- onto Ag(111) starting at more positive potentials than –0.56 V *vs.* SHE;[7,15] thus in the *in situ* STM investigations, competitive adsorption of iodide and hydroxide anions, influencing the potential of stable iodide adlayer formation, was possible. Considering results for the HI solution,[8] in which the peaks of iodide adsorption/desorption were not seen (they were overridden by hydrogen evolution), while the adlayer $(\sqrt{3}\times\sqrt{3})$R30° was detected by *in situ* STM at the potential of hydrogen evolution (–0.76 V *vs.* SHE), it seems that the difference between the previous and present results could be the consequence of both the above-mentioned reasons. Hence, it could be stated that although by the presented analysis it is not possible to obtain information about the exact structure of the adsorbed adlayers, valuable information concerning their adsorption kinetics could be obtained.

TABLE I. Results of the fitting peaks presented in Fig. 3 by Frumkin adsorption isotherms

Peak	f	$K_{ads,\theta\to0}$	ΔG_{ads} / kJ mol^{-1}
A	9.1	9.4×10^{20}	–119.8
B	–4.3	1.1×10^{6}	–34.5
A1	–1.6	6.6×10^{19}	–113.2
A2	1.5	3.7×10^{19}	–111.8
A3	–1.7	3.7×10^{16}	–94.6
A4	–4.5	2.6×10^{15}	–88.1

Cadmium UPD from 0.05 M CdI_2 + 0.1 M NaI

Since both ions, Cd^{2+} and I^- adsorb with the formation of ordered structures, this system is very convenient to investigate the influence of anion adsorption on cation adsorption. The process of Cd UPD onto Ag(111) in the presence of iodide anions was investigated in this work for the first time by the cyclic voltammetry and potentiostatic pulse techniques.

The CVs of Ag(111) recorded at a sweep rate of 100 mV s^{-1} in the absence (solid line) and presence of CdI_2 in the solution (dotted line) are shown in Fig. 4a. As can be seen, the UPD of Cd starts at about –0.25 V with a sharp increase in the cathodic current density, while the shape of the CV at more positive potentials only slightly changes and still shows the sharp peak of the phase transition of the $(\sqrt{3}\times\sqrt{3})$R30° iodide adlayer into the rotated hexagonal $(\sqrt{3}\times\times\sqrt{3})$R(30°+$\alpha$°) phase. The slightly different shape of this peak is most probably the consequence of the presence of Cd^{2+} in the double layer. The shape and position of this peak does not depend on the cathodic potential limit. Hence, al-

though the process of Cd adsorption/desorption (UPD) occurs at a more negative potential of –0.25 V, after Cd desorption, the $(\sqrt{3}\times\sqrt{3})$R30° adlayer of iodide still remains adsorbed on the Ag(111) surface and its transformation into the $(\sqrt{3}\times\sqrt{3})$R(30°+α°) phase occurs at the same potential as in the absence of Cd^{2+}. If the anodic limit is set to a more positive value, a well-defined nucleation loop of AgI formation and dissolution was detected, Fig. 4b.

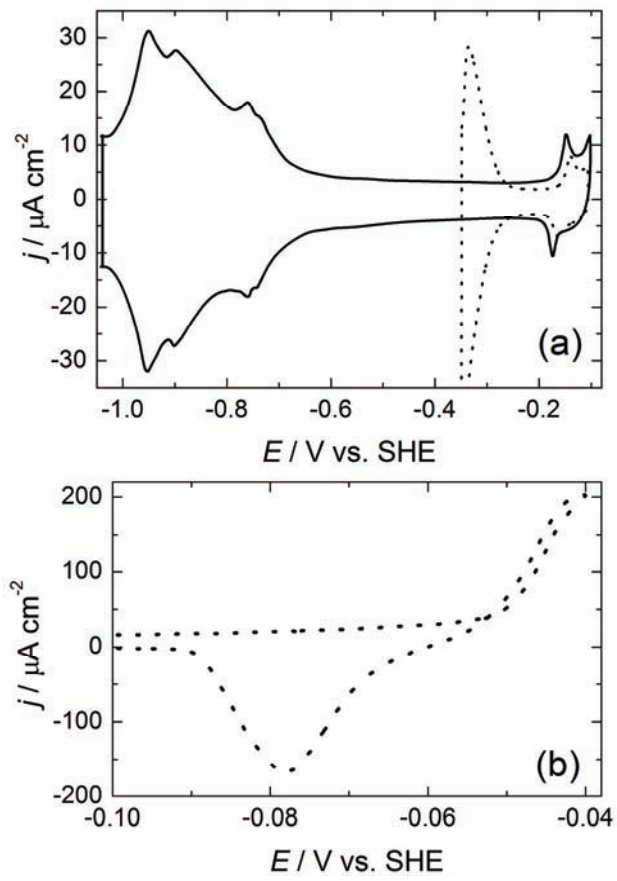

Fig. 4. a) CV of Ag(111) recorded at a sweep rate v = 100 mV s^{-1} in a solution of 0.1 M NaI (solid line) and in a solution containing 0.1 M NaI + 0.05 M CdI_2 (dotted line); b) CV of AgI formation and reduction recorded at a sweep rate v = 100 mV s^{-1} in the solution containing 0.1 M NaI + 0.05 M CdI_2.

In order to obtain much better insight into the UPD process, CVs were recorded at a low sweep rate of 5 mV s^{-1}. The corresponding CVs and Q *vs.* E dependences are presented in Figs. 5a and 5b, respectively. Three cathodic potential limits were set: one after the first peak C (solid line), one after the second peak D

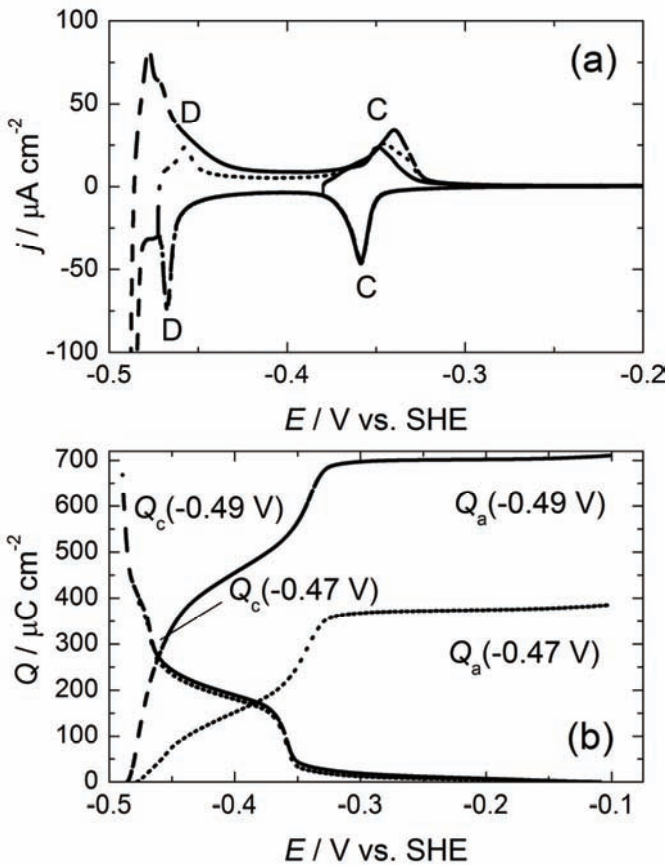

Fig. 5. a) CVs of the process of UPD of Cd onto Ag(111) recorded at a sweep rate v = 5 mV s^{-1} in the solution containing 0.1 M NaI + 0.05 M CdI_2: cathodic potential limit –0.38 (solid line), –0.47 (dotted line) and –0.49 V (dashed line); b) corresponding cathodic (Q_c) and anodic (Q_a) charges as a function of potential obtained by integration of the CVs presented in (a).

(dotted line) and one at –0.49 V (dashed line). The corresponding *Q vs. E* dependences, obtained for cathodic limits of –0. 47 and –0.49 V clearly indicate that the charge obtained for peak C (inflection point at Q_c *vs. E* at around –0. 36 V) amounts to ≈ 150 μC cm^{-2}, confirming the formation of the $(\sqrt{3}\times\sqrt{3})$R30° structure of Cd. In order for Cd to occupy the same $(\sqrt{3}\times\sqrt{3})$R30° sites, all of the iodide ad-atoms must first be desorbed from the (111) face of silver, contributing with an additional charge[1–8] of approximately 74 μC cm^{-2} (since a small charge was exchanged during the rearrangement of this ordered structure into randomly arranged adsorbed anions) to the 149 μC cm^{-2} cathodic charge associated with the adsorbed $(\sqrt{3}\times\sqrt{3})$R30° Cd structure.[11] The results presented in Fig. 5b clearly show that this was not the case since the charge attributed to the early stage of Cd UPD is about 150 μC cm^{-2}, which is quite close to the theo-

retical charge required for the ($\sqrt{3}\times\sqrt{3}$)R30° Cd structure (assuming complete charge transfer between Cd and Ag). Based on these results, it is obvious that desorption of iodide ad-atoms does not occur during Cd UPD, but they become replaced by cadmium ad-atoms, remaining adsorbed onto Cd layer and/or in between the adsorbed Cd ad-atoms. The sharp increase in the cathodic charge between –0.47 and –0.49 V overcomes the charge needed for the formation of a close packed monolayer (≈ 450 μC cm^{-2}) of Cd (Q_c(–0.49 V) and Q_a(–0.49 V) curves of Fig. 5b), indicating alloying of Ag and Cd,[9–11] as well as 3D deposition of Cd. Since the process of alloying has already been investigated in sulfates[9,10] and chlorides[11] containing solution, the intention in the present study was to investigate more closely the processes occurring under peaks C and D. In the first instance, by considering the shape of the CVs shown in Fig. 5a, it is clear that the anodic peaks are composed of more than one peak, while for cathodic peaks, it appears that they could be fitted with one peak only. The results of the PeakFit analysis for both the cathodic and anodic peaks are presented in Figs. 6–6c and 7a–7c, respectively. Since the current density between cathodic and anodic peaks C and D was not small as the one before the peak C (representing the double layer charging current density), it was decided to correct these voltammograms for the base line in order to avoid the influence of all the processes that are not represented by peaks C and D (replacement of ad-atoms, double layer charging, exchange of anions in the inner and outer Helmoholtz layer, *etc*.) and the correction for the base line is presented in Fig. 6a for the cathodic CV and in Fig. 7a for the anodic CV. As can be seen in Fig. 6b, the cathodic peaks C and D are composed of two peaks each, 1 (dashed line), 2 (dash-dot-dot line), 3 (dash-dot line) and 4 (dotted line), respectively. By the same procedure as in the previous analysis, adsorption isotherms (θ *vs. E* dependences) for all four peaks were obtained and fitted with the Frumkin adsorption isotherm (Eq. (1)). The experimental points are presented with squares, circles, and triangles, while the corresponding fitting results are presented by dashed, dotted, dash-dot and dash-dot-dot lines in Fig. 6c. The results of the fitting procedure are given in Table II. As can be seen, all peaks are characterized by the negative values of the interaction parameter *f*, indicating that the UPD in all cases is characterized by attractive lateral interaction between the adsorbed cadmium ad-atoms. This value for peaks 1, 3 and 4 overcomes the critical one of –4, confirming phase transition process. These results are in good agreement with the findings of other authors[9–11] that peak C represents phase transition into the ($\sqrt{3}\times\sqrt{3}$)R30° ordered Cd structure, while under peak D, phase transition of this structure into a close packed monolayer occurs. However, the shape of peak C, as well as the shape of a whole CV, changes in dependence of the presence of sulfates,[9,10] chlorides[11] and iodides. In sulfate and chloride electrolytes, peak C is characterized with a broad (broader in sulfate than in chloride) and a sharp peak. The broad peak corresponds to the random ad-

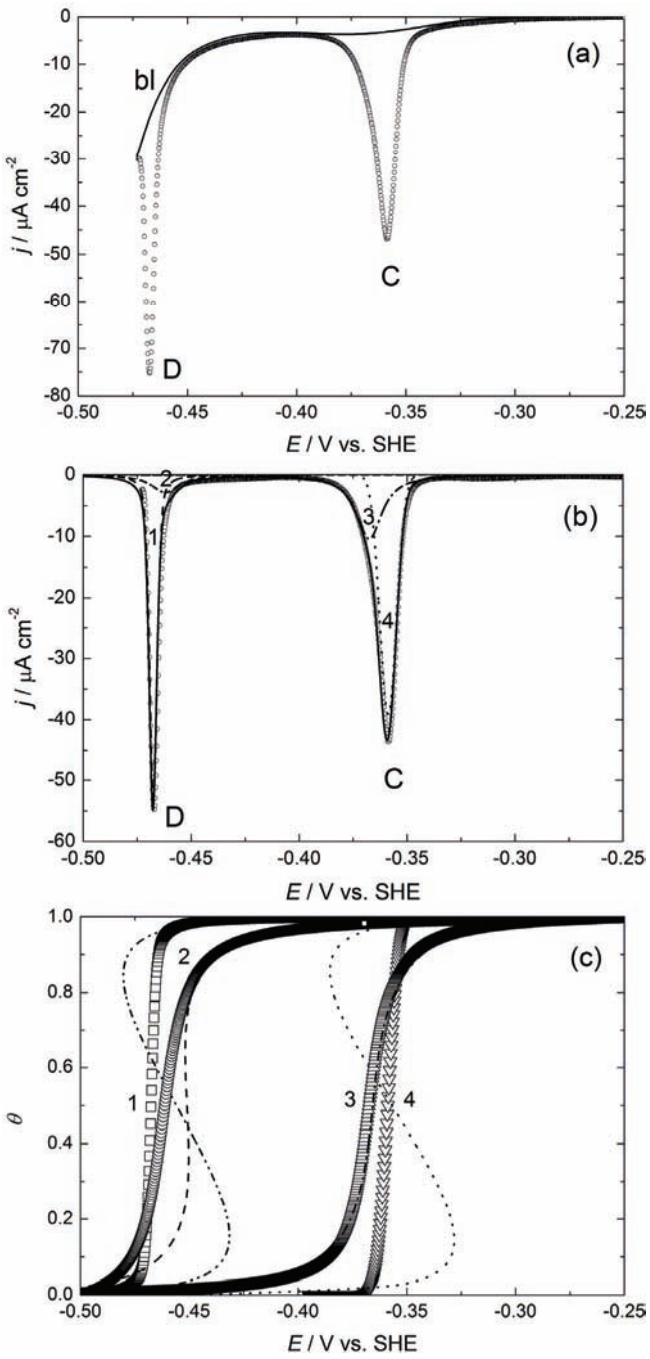

Fig. 6. a) Cathodic part of the CV presented in Fig. 5a: experimental points (○) and corresponding baseline (bl – solid line) – cathodic potential limit –0.47 V; b) cathodic part corrected for the base line; ○ – experimental curve; solid line – curve obtained by the PeakFit procedure; all peaks obtained by this procedure are marked with 1 (dashed line), 2 (dash-dot-dot line), 3 (dash-dot line), and 4 (dotted line); c) adsorption isotherms obtained by analysis of the corresponding peaks in (b): □ – experimental curve for peak 1; dash-dot--dot line – fitting curve; ○ – experimental curve for peak 2; dashed line – fitting curve; △ – experimental curve for peak 3; dash-dot line – fitting curve; ▽ – experimental curve for peak 4; dotted line – fitting curve.

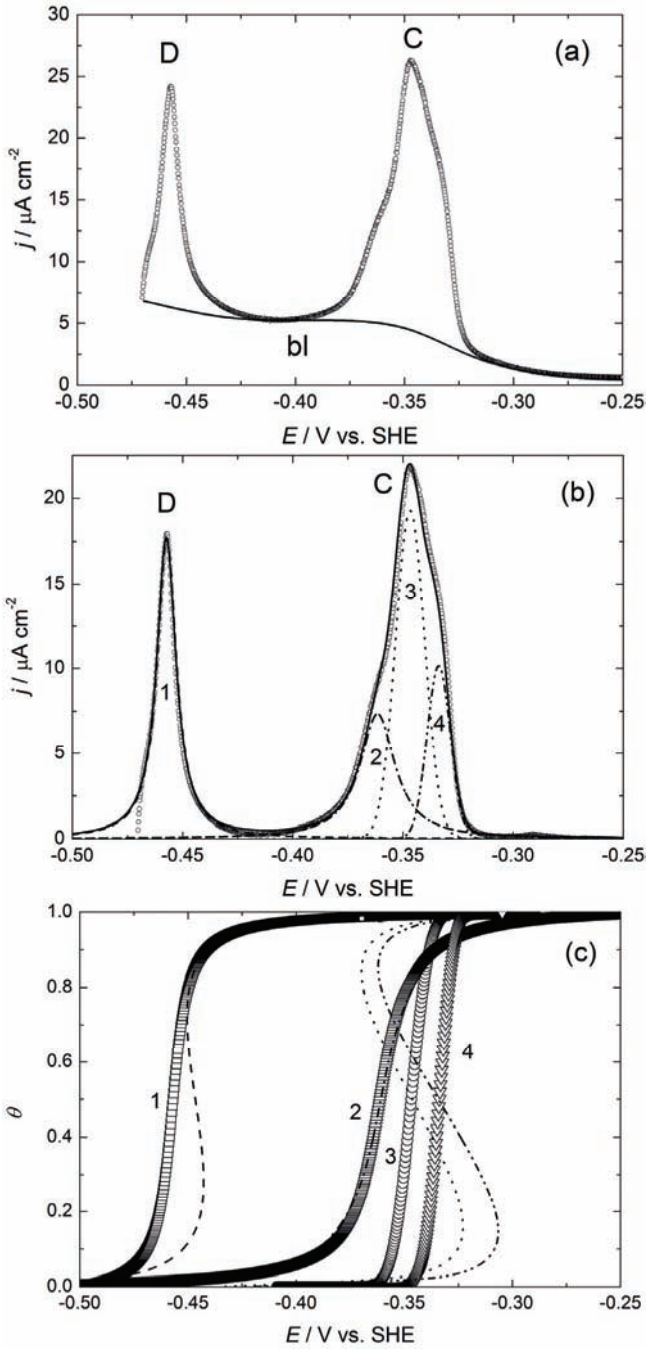

Fig. 7. a) Anodic part of the CV presented in Fig. 5a: experimental points (○) and corresponding baseline (bl – solid line) – cathodic potential limit –0.47 V; b) anodic part corrected for the base line; ○ – experimental curve; solid line – curve obtained by the PeakFit procedure; all peaks obtained by this procedure are marked with 1 (dashed line), 2 (dash-dot line), 3 (dotted line), and 4 (dash-dot-dot line); c) adsorption isotherms obtained by analysis of the corresponding peaks in (b): □ – experimental curve for peak 1; dashed line – fitting curve; △ – experimental curve for peak 2; dash–dot line – fitting curve; ○ – experimental curve for peak 3; dotted line – fitting curve; ▽ – experimental curve for peak 4; dash--dot-dot line – fitting curve.

sorption of Cd (the value of f is positive), while the sharp one represents phase transition into the ($\sqrt{3}\times\sqrt{3}$)R30° ordered Cd structure ($f \leq -4$). In both solutions, anions (sulfate or chloride) are already adsorbed on the Ag(111) surface when the UPD of Cd commences (peak C). The adsorbed adlayer of chlorides is known to transform from ($\sqrt{3}\times\sqrt{3}$)R30° chloride adlayer into a randomly adsorbed chloride adlayer just before the commencement of Cd UPD.[1,6,11,13,16–20] The structure of adsorbed sulfate ad-atoms is unknown and there are only three papers dealing with the structure and coverage of the adsorbed sulfate onto Ag(111).[21–23] Schweizer and Kolb[21] detected a $c(3\times3\sqrt{3})$ ordered sulfate structure on Ag(111), but this "structure was found to be stable only for a relatively short time (about 1 h) at potentials between –0.25 and 0.05 V *vs*. SCE". These experiments were performed in 0.1 M H_2SO_4, in which HSO_4^- prevail, while most of the Cd UPD experiments were performed in solutions of high concentrations of Na_2SO_4, in which SO_4^{2-} prevail.[9,10] In a previous paper,[23] it was found that in 0.2 M Na_2SO_4, the adsorption of sulfates onto Ag(111) is characterized by two peaks at potentials between –0.45 and –0.15 V *vs*. SHE. The adsorbed sulfate structure is less dense than that expected for a sulfate monolayer and the process of sulfate adsorption follows a Frumkin adsorption isotherm with a high positive value of the interaction parameter f = 16.5, indicating repulsive lateral interaction between the adsorbed anions,[23] *i.e.*, randomly distributed sulfate ad-atoms (it was also found that complete charge transfer occurs). Hence, it could be concluded that in both cases, the Cd UPD starts on the Ag(111) surface which is not covered with adsorbed anions characterized by attractive forces between each other. The beginning of the Cd UPD in sulfate solution is placed at around –0.17 V *vs*. SHE and in chloride solution at around –0.20 V *vs*. SHE. In the case of iodide solution, the ($\sqrt{3}\times\sqrt{3}$)R30° iodide adlayer is on the surface[8] when the Cd UPD process commences at around –0.34 V *vs*. SHE. From this behavior, it is obvious that the Cd UPD moves to more negative potentials with increasing attractive forces between the adsorbed anions, *e.g.*, more energy is required to replace the adsorbed iodides with Cd cations. Simultaneously, peak C, representing this process, changes its shape from a combination of a broad and sharp peak to one sharp peak only. As can be seen in Fig. 6b, this process is actually the simultaneous occurrence of two processes, both characterized with attractive forces between the adsorbed ad-atoms (Table II). It is not possible to determine the origin of both peaks. Peak 4 corresponds to the formation of the ($\sqrt{3}\times\sqrt{3}$)R30 structure of the adsorbed Cd, while peak 3 might be ascribed to the rearrangement of the ($\sqrt{3}\times\sqrt{3}$)R30° iodide adlayer into some undefined, ordered structure on top of the Cd adlayer and/or in between the Cd ad-atoms, or to a continuation of the formation of the ($\sqrt{3}\times\sqrt{3}$)R30° structure of the adsorbed Cd. A similar supposition could be made for peak D, corresponding to the formation of a close packed Cd monolayer, with peak 1 representing the phase tran-

sition of the ($\sqrt{3}\times\sqrt{3}$)R30° Cd adlayer into a close packed monolayer and peak 2 representing a rearrangement of the adsorbed structure of iodide on top of a Cd monolayer, or a continuation of the process of close packed Cd monolayer formation. Slightly different results were obtained by the deconvolution of the anodic peaks C and D presented in Figs. 7a–7c. It appears that peak 1 corresponds to the phase transition of the Cd monolayer into a ($\sqrt{3}\times\sqrt{3}$)R30° Cd adlayer, while peaks 2 and 3 correspond to the process of desorption of the ($\sqrt{3}\times\sqrt{3}$)R30° Cd adlayer. This is consistent with the observations of Stuhlmann *et al.*[24] that the Cd adlayer is stabilized by chloride, thereby forming a $CdCl_2$-like layer on the copper surface. It appears that in the case of Ag(111) in iodide solution, the cadmium adlayer replaces the surface iodide, with the iodide remaining adsorbed on the Cd monolayer. Hence, peak 4 could be ascribed to the formation of ($\sqrt{3}\times\sqrt{3}$)R30° iodide adlayer on the Ag(111) surface, since it is characterized with an f value more negative than the critical one for phase transition (f = –8.0, Table II), as well as with the lowest value (1.3×10^8) of adsorption equilibrium constant for all peaks reflecting the UPD process (Table II). Taking into account that the ($\sqrt{3}\times\sqrt{3}$)R30° iodide adlayer in the absence of Cd ad-atoms is formed at a potential around –0.75 V (Fig. 3), it seems reasonable that its formation at more positive potentials should be faster, which is reflected by the high negative value of f and the small value of the equilibrium adsorption constant. It should be stated here that it is quite possible that Cd and iodide ad-atoms form some kind of mixed structures in the potential region between and around peaks C and D, as was the case with the Tl and bromide ad-atoms,[25] but to prove this it would be necessary to perform *in situ* X-ray investigations with accelerated electrons.

TABLE II. Results of fitting the peaks C and D presented in Figs. 6 and 7 by Frumkin adsorption isotherms

Cathodic peak	f	$K_{ads,\theta\to0}$	ΔG_{ads} / kJ mol^{-1}
1	–7.6	1.7×10^{10}	–52.1
2	–4.3	7.4×10^{10}	–55.6
3	–3.3	4.6×10^{9}	–71.6
4	–8.1	3.0×10^{8}	–61.3
Anodic peak			
1	–5.0	4.5×10^{10}	–62.1
2	–2.7	5.2×10^{9}	–57.2
3	–7.5	2.7×10^{8}	–51.7
4	–8.0	1.3×10^{8}	–49.9

Considering the adsorption isotherms presented in Figs. 3b (B), 3c (A4), 6c (1, 2 and 4) and 7c (1, 3 and 4), it can be seen that the fitting curves deviate from the experimental ones, having an "S" shape. This is typical for f values more negative than –4. The experimental curves are characterized with a sudden increase of coverage with potential, while the fitted ones show that the "coverage in-

creases with decreasing potential". Such a behavior obviously does not represent the physical reality of the process.[14] Hence, for all isotherms with $f \leq -4$, the experimental curves would show sudden transition from low to high coverage, while the fitted ones will possess an "S" shape. Complete discontinuity on the isotherms was discussed previously in more details (Fig. 15 in Ref. 12). It is obvious that in the cyclic voltammetry experiments, particularly those recorded at sweep rates higher than 1 mV s^{-1}, such discontinuity cannot be obtained. It is possible to record discontinuous isotherm only with pulse experiments if the potential step is about 1 mV, as shown in Fig. 5 of Ref. 26 for the Pb UPD onto Ag(111).

The UPD of Cd was also investigated by the potentiostatic pulse technique. The initial potential was set at –0.1 V and cathodic pulses were applied in a sequence of 10 mV starting from –0.3 V. The duration of the cathodic pulses was either 40 or 50 ms and then an anodic pulse back to the initial potential was applied. Since the anodic *j–t* transients were much better defined, they were used for further analysis. The anodic *j–t* transients for most of the applied potentials are presented in Fig. 8. As can be seen, monotonously falling transients of short duration (up to 2 ms) were recorded for potentials more positive and in the region of the beginning of peak C (from –0.30 to –0.35 V). For cathodic potentials more negative than the potentials of peak C (from –0.37 to –0.41 V), the shape of the anodic *j–t* transients changed indicating the occurrence of the Cd UPD process and a much larger charge was recorded for these pulses. At more negative pulse potentials (from –0.45 to –0.49 V), two waves could be detected on the anodic *j–t* transients, indicating that two processes occurred (desorption of both the Cd monolayer and the $(\sqrt{3}\times\sqrt{3})$R30° Cd adlayer). By integration of the anodic *j–t* transients, the *Q vs*. *E* dependence was obtained, which is presented in Fig. 9 (the same dependence was obtained by the integration of the cathodic *j–t* transients, not shown here). This dependence is characterized by three inflection points: the first one (I) corresponding to the beginning of the Cd UPD process, the second one (II) corresponding to the formation of a $(\sqrt{3}\times\sqrt{3})$R30° Cd adlayer (at around 150 μC cm^{-2}) and the third one (III) reflecting the beginning of the formation of a close packed Cd monolayer. The charge required for the formation of the close packed Cd monolayer is reached at a potential of –0.49 V. Comparing the shape of *Q vs*. *E* dependence obtained by the analysis of potentiostatic pulse results (Fig. 9) with the one obtained by integration of the CV recorded at a sweep rate of 5 mV s^{-1} (Fig. 5b, Q_c(–0.49 V)), it can be seen that they are practically identical.

Finally, as stated for iodide adsorption, the presented analysis cannot give information about the exact structure of the adsorbed adlayers but valuable information concerning their adsorption kinetics could be obtained. In the case of Cd

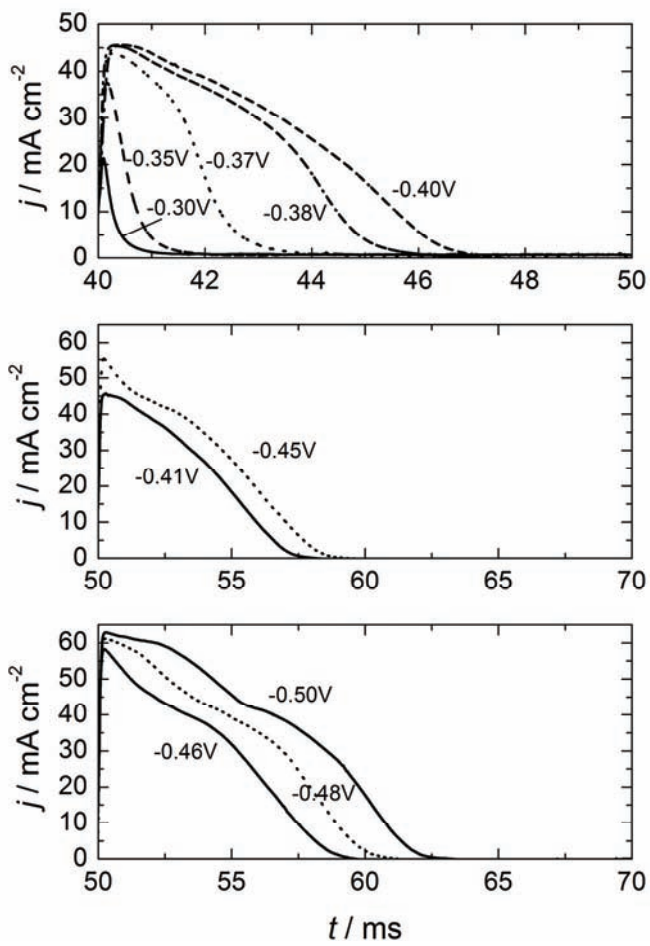

Fig. 8. Anodic *j*–*t* transients (potentials were stepped from the applied cathodic potentials to a potential of –0.1 V) recorded after applying pulse potentials at the values marked in the Figure.

UPD in the presence of iodide anions, the question arises whether it would be possible to detect the $(\sqrt{3}\times\sqrt{3})$R30° Cd adlayer and close packed Cd monolayer if some ordered structure of iodide ad-atoms is formed on top of the Cd layer. For sulfate solution,[10] as well as for chloride solution,[24] this was possible since the formation of the $(\sqrt{3}\times\sqrt{3})$R30° Cd adlayer commences on an (111) surface covered with randomly adsorbed anions, and it seems unrealistic to expect an ordered structure of these anions on top of the Cd layer. In the case of iodide anions, the formation of the $(\sqrt{3}\times\sqrt{3})$R30° Cd adlayer starts on an Ag(111) surface covered with the same structure of adsorbed iodide and it is possible that the same, or a similar ordered structure of iodide, could be formed on top of the Cd adlayer and/or in between the Cd ad-atoms, which would make the determination

of the Cd under-layer difficult by *in situ* STM. According to the STM analysis of Pd monolayer formation onto Pt(111)[27] from a sulfate containing electrolyte, it appears that the ordered sulfate structure ($\sqrt{3}\times\sqrt{7}$)R19.1° adsorbed onto the Pd monolayer masks the structure of the under-layer (Pd monolayer). Hence, if something similar occurs in the case of Cd UPD onto Ag(111) in the presence of iodide anions, it would be (most likely) possible to detect some adlayer of iodide ad-atoms only on the bare Ag(111) surface (between the adsorbed Cd ad-atoms in the ($\sqrt{3}\times\sqrt{3}$)R30° structure). This is obviously a problem which deserves attention and it is believed that someone having the possibility to perform *in situ* STM measurements on this system (which is not the case for us), should investigate this process.

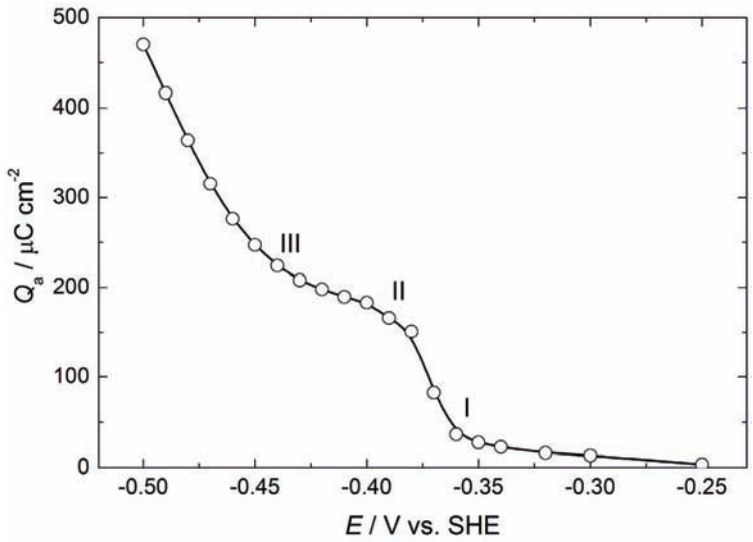

Fig. 9. Charge *vs.* potential curve obtained by integration of the anodic *j–t* transients presented in Fig. 8.

CONCLUSIONS

From the results presented in this paper, it could be concluded that the process of iodide adsorption is characterized by one broad and one sharp peak. The broad peak could be deconvoluted into five peaks: A, A1–A4. Peak A represents the random adsorption of iodide anions, mainly at the monoatomic steps as favorable locations for adsorption, while peaks A1, A3 and A4 are characterized by negative values of *f*, indicating attractive lateral interaction between the adsorbed anions. Only one peak, A4, possesses a value of $f < -4$, indicating a phase transition process. Peak B also corresponds to the phase transition process of the ($\sqrt{3}\times\sqrt{3}$)R30° iodide adlayer into a rotated hexagonal ($\sqrt{3}\times\sqrt{3}$)R(30°+α°) phase.

The adsorption/desorption process of cadmium cations in the presence of iodides is characterized by two main peaks, each of them being composed of two or three peaks with negative values of *f*. By analysis of the charge *vs*. potential dependences obtained either from the CVs or the current transients on potentiostatic pulses, it was concluded that the adsorbed iodide anions did not undergo desorption during the process of Cd UPD, but became replaced by Cd ad-atoms and remained adsorbed on top of a Cd layer and/or in between Cd ad-atoms.

Acknowledgement. The authors are indebted to the Ministry of Science and Technological Development of the Republic of Serbia (Project No. 172054) for the financial support of this work.

И З В О Д

ПРОЦЕСИ АДСОРПЦИЈЕ/ДЕСОРПЦИЈЕ ЈОДИДА И КАТЈОНА КАДМИЈУМА НА Ag(111)

ВЛАДИМИР Д. ЈОВИЋ и БОРКА М. ЈОВИЋ

Институт за мултидисциплинарна истраживања, п. пр. 33, 11030 Београд

У овом раду су испитивани процеси адсорпције/десорпције јодида и катјона кадмијума у присуству јодида на Ag(111). Показано је да су оба процеса комплексна и да су окарактерисани са по неколико пикова на цикличним волтамограмима. Помоћу PeakFit анализе добијених волтамограма и накнадног фитовања сваког регистрованог пика Фрумкиновом адсорпционом изотермом одређени су параметри процеса адсорпције, фактор интеракције (*f*) и Гибсова енергија адсорпције (ΔG_{ads}) за сваку адсорбовану фазу. У случају адсорпције јодида четири пика су поседовала негативне вредности *f*, указујући на привлачне силе између адсорбованих анјона, док су вредности *f* за два пика биле негативније од –4 што је била потврда одигравања процеса фазне трансформације при адсорпцији јодида. Процес адсорпције/десорпције катјона кадмијума (UPD) у присуству јодида окарактерисана је са два главна пика, при чему је сваки пик био састављен од два или три пика са вредностима *f* негативнијим од –4. Анализом зависности наелектрисања од потенцијала закључено је да се адсорбовани јодиди не десорбују при процесу адсорпције катјона кадмијума, већ их на површини монокристала замењују ад-атоми кадмијума док јодиди остају адсорбовани на слоју адсорбованог кадмијума и/или између адсорбованих ад-атома кадмијума.

(Примљено 1. јула, ревидирано 23. августа 2010)

REFERENCES

1. G. N. Salaita, F. Lu, L. Laguren-Davison, A. T. Hubbard, *J. Electroanal. Chem.* **229** (1987) 1
2. J. H. Schott, H. S. White, *J. Phys. Chem.* **98** (1994) 291
3. J. H. Schott, H. S. White, *J. Phys. Chem.* **98** (1994) 297
4. J. H. Schott, H. S. White, *Langmuir* **10** (1994) 486
5. M. Kawasaki, H. Ishii, *Langmuir* **11** (1995) 832
6. M. L. Foresti, G. Aloisi, M. Innocenti, H. Kobayashi, R. Guidelli, *Surf. Sci.* **335** (1995) 241
7. K. J. Stevenson, X. Gao, D. W. Hatchett, H. S. White, *J. Electroanal. Chem.* **447** (1998) 43
8. T. Yamada, K. Ogaki, S. Okubo, K. Itaya, *Surf. Sci.* **369** (1996) 321

9. H. Bort, K. Jüttner, W. J. Lorenz, G. Staikov, *Electrochim. Acta* **28** (1983) 993
10. S. G. Garcia, D. R. Salinas, G. Staikov, *Surf. Sci.* **576** (2005) 9
11. V. D. Jović, B. M. Jović, *Electrochim. Acta* **47** (2002) 1777
12. J. N. Jovićević, V. D. Jović, A. R. Despić, *Electrochim. Acta* **29** (1984) 1625
13. B. M. Jović, V. D. Jović, D. M. Dražić, *J. Electroanal. Chem.* **399** (1995) 197
14. E. Gileadi, *Electrode Kinetics for Chemists, Chemical Engineers, and Materials Scientists*, VCH Publishers Inc., New York, 1993, p. 305
15. B. M. Jović, V. D. Jović, G. R. Stafford, *Electrochem. Commun.* **1** (1999) 247
16. M. L. Foresti, M. Innocenti, F. Forni, R. Guidelli, *Langmuir* **14** (1998) 7008
17. M. Innocenti, M. L. Foresti, A. Fernandez, F. Forni, R. Guidelli, *J. Phys. Chem. B* **102** (1998) 9667
18. M. S. Zei, *J. Electroanal. Chem.* **308** (1991) 295
19. D. D. Sneddon, A. A. Gewirth, *Surf. Sci.* **343** (1995) 185
20. D. D. Sneddon, D. M. Sabel, A. A. Gewirth, *J. Electrochem. Soc.* **142** (1995) 3027
21. M. Schweizer, D. M. Kolb, *Surf. Sci.* **544** (2003) 93
22. S. Smolinski, P. Zelenay, J. Sobkowski, *J. Electroanal. Chem.* **467** (1998) 41
23. B. M. Jović, D. M. Dražić, V. D. Jović, *J. Serb. Chem. Soc.* **64** (1999) 539
24. C. Stuhlmann, Z. Park, C. Bach, K. Wandelt, *Electrochim. Acta* **44** (1998) 993
25. J. X. Wang, I. K. Robinson, R. R. Adžić, *Surf. Sci.* **412/413** (1998) 374
26. V. D. Jović, J. N. Jovićević, A. R. Despić, *Electrochim. Acta* **30** (1985) 1455
27. R. Hoyer, L. A. Kibler, D. M. Kolb, *Electrochim. Acta* **49** (2003) 63.